

Long-range entanglement in the XXZ Heisenberg spin chain after a local quench

Jie Ren^{1*} and Shiqun Zhu^{2†}

¹*Department of Physics and Jiangsu Laboratory of Advanced Functional Materials,
Changshu Institute of Technology, Changshu, Jiangsu 215500, China*

²*School of Physical Science and Technology,
Suzhou University, Suzhou, Jiangsu 215006, China*

(Dated: November 15, 2018)

Abstract

The long-range entanglement dynamics of an one-dimensional spin-1/2 anisotropic XXZ model are studied using the method of the adaptive time-dependent density-matrix renormalization-group. The long-range entanglement can be generated when a local quench on one of boundary bonds is performed in the system. The anisotropic interaction has a strong influence both on the maximal value of long-range entanglement and the time of reaching the maximum long-range entanglement. The local coupling has a notable impact on the long-range entanglement, but it can be neglected in the time of reaching the maximal long-range entanglement.

PACS number: 03.67.Mn, 03.65.Ud, 75.10.Pq

Keywords: long-range entanglement, spin chain, adaptive time-dependent density-matrix renormalization-group

* E-mail: jren@cslg.edu.cn

† E-mail: szhu@suda.edu.cn

I. INTRODUCTION

Entanglement generation and distribution is one of the important problems in performing quantum-information tasks, such as quantum computation and quantum teleportation [1–3]. Many results showed that entanglement existed naturally in the spin chain when the temperature is at zero [4, 5]. It is discouraging that the entanglement in many spin systems is typically very short ranged. It exists only in the nearest neighbors and the next nearest neighbors [6]. It is interesting that some schemes for long-range entanglement, such as exploiting weak couplings of two distant spins to a spin chain were proposed [7–9]. These methods have limited thermal stability or very long time scale of entanglement generation. In recent years, many researches has shifted the focus of the study in the dynamics of entanglement [10–14]. The dynamics of long range entanglement are obtained by a time quench of magnetic field [15, 16]. The end-to-end entanglement can be shared across a chain of arbitrary range [10]. It is excited that the most common situation studies so far concerns a sudden quench of some coupling of the model Hamiltonian [17–19]. In Ref. [19], it showed that the long-range entanglement can be engineered by a non-perturbative quenching of a single bond in a Kondo spin chain with impurity. This is the first example that a minimal local action on a spin chain can generate long-range entanglement dynamically. It would be interesting to investigate the possibility of producing long-range entanglement in the XXZ Heisenberg spin chain without impurity.

It is well-known that the Hamiltonian of an opened chain of N spin-1/2 system with nearest-neighbor XXZ interaction is given by

$$H_0 = \sum_{i=1}^{N-1} J[S_i^x S_{i+1}^x + S_i^y S_{i+1}^y + \Delta S_i^z S_{i+1}^z], \quad (1)$$

where $S_i^\alpha (\alpha = x, y, z)$ are spin operators on the i -th site, N is the length of the spin chain. The parameter Δ denotes the couplings in the z -axis. This model can be realized in the Josephson-junction[20] and optical lattices[21, 22].

In the paper, the long-range entanglement in the XXZ Heisenberg spin chain after a local quench is investigated. An opened boundary condition (OBC) is assumed because the antiferromagnetic Heisenberg spin chain with OBC can be achieved artificially in the experiment [23], and the coupling $J = 1$ is considered for simplicity. In section II, the local quench is presented. The concurrence is used as a measurement of the entanglement. In

section III, a more general situation and a single quench and its effect on the end-to-end qubits entanglement are analyzed. The effects of the anisotropic interaction and system size on the end-to-end qubits entanglement is also studied. The robustness of the entanglement against an increase in temperature is investigated. A discussion concludes the paper.

II. LOCAL QUENCH AND ENTANGLEMENT MEASURE

In the paper, the system is assumed to be in the ground state G_{s_0} of H_0 initially. A local quench change of the coupling between the first qubit and the second qubit with the same anisotropy interaction Δ in Eq. (1) is performed. The Hamiltonian of the system modifies to

$$H_1 = J_1[S_1^x S_2^x + S_1^y S_2^y + \Delta S_1^z S_2^z] + \sum_{i=2}^{N-1} J[S_i^x S_{i+1}^x + S_i^y S_{i+1}^y + \Delta S_i^z S_{i+1}^z]. \quad (2)$$

Since $[H_0, H_1] \neq 0$, the the ground state G_{s_0} of H_0 is not one of the eigenstates of H_1 . The state of the system will evolve as

$$\psi(t) = \exp^{-iH_1 t} G_{s_0}. \quad (3)$$

In the paper, the concurrence is chosen as a measurement of the pairwise entanglement [3]. The concurrence C is defined as

$$C_{1,N} = \max\{\lambda_1 - \lambda_2 - \lambda_3 - \lambda_4, 0\}, \quad (4)$$

where the quantities $\lambda_i (i = 1, 2, 3, 4)$ are the square roots of the eigenvalues of the operator $\varrho = \rho_{12}(\sigma_1^y \otimes \sigma_N^y)\rho_{1,N}^*(\sigma_1^y \otimes \sigma_N^y)$. They are in descending order. The case of $C_{1,N} = 1$ corresponds to the maximum entanglement between the two qubits, while $C_{1,N} = 0$ means that there is no entanglement between the two qubits.

III. LONG-RANGE ENTANGLEMENT DYNAMICS

It is known that it is hard to calculate the dynamics of entanglement because of the lack of knowledge of eigenvalues and eigenvectors of the Hamiltonian. For models that are not exactly solvable, most of researchers resort to exact diagonalization to obtain the ground

state for small system size. The method is difficult to be applied for large system size $N > 20$. For a large system, the adaptive time-dependent density-matrix renormalization-group can be applied with a second order Trotter expansion of the Hamiltonian as described in [24, 25]. In order to check the accuracy of the results of the adaptive time-dependent density-matrix renormalization-group, the results of exact diagonalization can be considered as a benchmark for a small size system.

The numerical error of the adaptive time-dependent density-matrix renormalization-group comes from the discarded weight and the Trotter decomposition. The error of discarded weight is dependent on the data precision and truncated Hilbert space. The error of the Trotter decomposition is relied on Trotter slicing. In our numerical simulations a Trotter slicing $\delta t = 0.05$ and Matlab codes of the adaptive time-dependent density-matrix renormalization-group with double precision are performed with a truncated Hilbert space of $m = 100$. It turns out that a typically discarded weight of $\delta\rho \leq 10^{-8}$. The error of Trotter decomposition $\delta \propto (\delta t)^3$. These can keep the relative error δC in C below 10^{-3} for a chain of $N = 60$ sites with time $t \leq 50/J$.

In the adaptive time-dependent density-matrix renormalization-group, it is hard to calculate the reduced density matrix $\rho_{1,N}$. By making use of the relation between the correlation and the reduced density matrix, the reduced density matrix can be expressed as

$$\rho_{1,N} = \frac{1}{4}[I_{1,N} + \sum_{i,j=x,y,z} \langle \sigma_1^i \sigma_N^j \rangle \sigma_1^i \sigma_N^j], \quad (5)$$

where σ_k^α ($\alpha = x, y, z$) are Pauli operators and $I_{1,N}$ is identity matrix.

We obtain the reduced density matrix $\rho_{1,N}$ by Eq. (5), then calculate the entanglement between two-ends qubits. The end-to-end entanglement $C_{1,N}$ is plotted as a function of the anisotropic interaction Δ and time t with $J_1 = -0.01$ in Fig. 1(a). It is seen that the long-range entanglement $C_{1,N}$ can be generated after a short time. When the time t increases, the entanglement reaches the maximal value and then disappears quickly. That is, there is a peak in the entanglement. The peak of the end-to-end entanglement is plotted as a function of the anisotropic interaction Δ in Fig. 1(b). It is seen that the peak in long-range end-to-end entanglement increases with the anisotropic interaction Δ . It reaches the maximal value when the anisotropic interaction $\Delta = 1$ [26, 27]. With the anisotropic interaction Δ increases further, the height of the peak decreases.

The relation between the time of reaching the maximal end-to-end entanglement labeled by T_{max} and the anisotropic interaction Δ can be seen in the inset of Fig. 1(b). The time of reaching the maximal long-range entanglement decreases when the anisotropic interaction Δ increases, while they are also not a linear relationship. Similar to Refs. [10, 19], the system generates end-to-end entanglement periodically. In our simulations, the error of the simulations increases when the time increases. Since the coherent time of the system is not very long, the long-distance entanglement is not shown when the time $t > 50/J$. It is shown that a sharp drop of long-distance entanglement occurs at $\Delta = -0.5$. Furthermore, the time of the long-range entanglement reaching the maximal value goes up drastically. This is similar to the anomalous behavior appeared in Ref. [27].

The end-to-end entanglement $C_{1,N}$ is plotted as a function of the interaction J_1 and the time t with $\Delta = 1$ in Fig. (2). The size of the system $N = 20$ is chosen. It does not include the case of $J_1 = 0$. The long-range entanglement $C_{1,N}$ can be generated after a short time. There is a peak in $C_{1,N}$ when $C_{1,N}$ is plotted as a function of time t . It is seen that the influence of the coupling J_1 on the maximal long-range entanglement is relatively large. The peak of the end-to-end entanglement increases when the coupling interaction J_1 increases, and reaches the maximal value when $J_1 = -0.1$. It seems that the changing of local interaction from antiferromagnetic to ferromagnetic may enhance the entanglement creation [7]. When J_1 increases further to $J_1 > 0.32$, the long-range entanglement disappears. It is interesting that the coupling interaction J_1 has a relatively small impact on the time when the end-to-end entanglement generates and reaches the maximal value.

It is easy to obtain that $[H_0, \sum_{i=1}^N S_i^z] = [H_1, \sum_{i=1}^N S_i^z] = 0$. It means that the ground states of H_0 is a total singlet $S_{tot} = 0$. The Hamiltonian H_1 has invariant on every excitation subspaces. During the evolution, the boundary spin at $i = 2$ will have a strong tendency to form a singlet pair with its only nearest neighbor $i = 3$ on the right-hand side. This is similar for spin pairs (4, 5) and (6, 7),, etc. Then the two-end spin qubits form a singlet. The local interaction J_1 decides the ability of forming singlet for even bands. Thus, the long-distance entanglement creates.

The thermalization and relaxation during the period of generating long-distance entanglement are neglected because the dynamical time scale is quite short. When initial state is taken to be the relevant thermal state, the end-to-end entanglement is plotted as a function of temperature in Fig. 3 after bond quenching for different system sizes. It is shown that

the entanglement vanishes when $kT > 1.16$ with the size of $N = 8$, and $kT > 1.06$ with the size of $N = 10$. It seems that our scheme is quite robust against temperature and is similar to that in Ref. [19]. The initial thermal state does not have long-distance entanglement in Eq. (1), but the energy gap between the ground state and the first and other excited states are larger than the system with impurity. This leads to our scheme is quite robust against temperature.

It is interesting to investigate the long-range entanglement creation even for very long chain of large size. The maximal value of the end-to-end entanglement $C_{1,N}$ is plotted as a function of the size of the system for different anisotropic interaction Δ and different interaction J_1 in Fig. 4(a). It is found that the maximal value of the end-to-end entanglement $C_{1,N}$ decreases when the size of system increases. When the anisotropic interaction $\Delta = 1$ and the interaction $J_1 = -0.1$, the maximal value is 0.5481 for $N = 40$ and 0.4547 for $N = 60$. It is shown that the maximal value of the end-to-end entanglement label by $\xi(N)$ is given by [10]

$$\xi(N) \simeq 1.35N^{-1/3}. \quad (6)$$

In Ref. [10], $\xi(40) \simeq 0.3947$ for $N = 40$, and $\xi(60) \simeq 0.3448$ for $N = 60$. While in the Kondo regime, $\xi(40)$ can be as large as 0.7 for $N = 40$. It seems that our results are also quite good. The long distance entanglement can be obtained by performing a local quench in either one of two boundary bands. The time of reaching the maximal end-to-end entanglement labeled by T_{max} is plotted as a function of the size N of the system for different anisotropic interaction Δ and different interaction J_1 in Fig. 4(b). The time of the end-to-end entanglement reaching the maximal value T_{max} is linear increase when the size N increases [10, 27]. It is seen that the slope of the line is almost dependent on the anisotropic interaction Δ .

In the paper, adiabatic quenches are studied and the decoherence effects in the system are ignored. It is noted that the XXZ spin chains can be realized in the Josephson-junction array [20] and optical lattices [21, 22]. In Josephson-junction array, the interactions and the anisotropy can be modulated by varying voltages [28]. The Josephson-junction array system does not have significant decoherence over our time-scales ($T_{max} \simeq N/J$) [29]. The anisotropic interaction quenches can be achieved successfully with long decoherence time in the optical lattices experiment [22].

IV. DISCUSSION

By using the method of the adaptive time-dependent density-matrix renormalization-group, the time evolution of the entanglement in a one-dimensional spin-1/2 anisotropic XXZ model is investigated when a local quench is performed in the system. The local quench is a abrupt change of interaction between the first qubit and the second qubit. The dynamics of pairwise entanglement between the two ends qubits in the spin chain is studied. The entanglement of the two-ends spin qubits can be created after the local quench is performed. The time when the long-range entanglement generates decreases in a nonlinear manner with the anisotropic interaction increases. It reaches the maximal value when the anisotropic interaction $\Delta = 1$. The maximal value of the end-to-end entanglement increases with the coupling interaction J_1 increases, and reaches the maximal when $J_1 = -0.1$. It is interesting that the coupling interaction has a relatively small impact on the time when the long-range entanglement reaches the maximal value. This phenomenon may be used to control the dynamics of the entanglement by varying the anisotropic interaction and the local quench interaction of the Heisenberg spin chain.

Acknowledgments

It is a pleasure to thank Yinsheng Ling and Yinzhong Wu for their many helpful discussions. The financial support from the National Natural Science Foundation of China (Grant No. 10774108) is gratefully acknowledged.

-
- [1] M. A. Nielsen and I. L. Chuang, *Quantum Computation and Quantum Information* (Cambridge University Press, Cambridge, England, 2000).
 - [2] C. H. Bennett, G. Brassard, C. Crepeau, R. Jozsa, A. Peres, and W. K. Wootters, *Phys. Rev. Lett.* **70**, 1895 (1993).
 - [3] W. K. Wootters, *Phys. Rev. Lett.* **80**, 2245 (1998).
 - [4] T. J. Osborne and M. A. Nielsen, *Phys. Rev. A* **66**, 032110 (2002).
 - [5] A. Osterloh, L. Amico, G. Falci, and R. Fazio, *Nature* **416**, 608 (2002).
 - [6] L. Amico, R. Fazio, A. Osterloh, and V. Vedral, *Rev. Mod. Phys.* **80**, 517 (2008).
 - [7] L. C. Venuti, C. D. E. Boschi, and M. Roncaglia, *Phys. Rev. Lett.* **96**, 247206 (2006).

- [8] L. C. Venuti, S. M. Giampaolo, F. Illuminati, and P. Zanardi, *Phys. Rev. A* **76**, 052328 (2007).
- [9] S. M. Giampaolo and F. Illuminati, *New J. Phys.* **12**, 025019 (2010).
- [10] S. Bose, *Phys. Rev. Lett.* **91**, 207901 (2003).
- [11] M. J. Hartmann, M. E. Reuter, and M. B. Plenio, *New J. Phys.* **8**, 94 (2006).
- [12] Y. Li, T. Shi, B. Chen, Z. Song, and C.-P. Sun, *Phys. Rev. A* **71**, 022301 (2005).
- [13] A. Wójcik, T. Łuczak, P. Kurzyński, A. Grudka, T. Gdala, and M. Bednarska, *Phys. Rev. A* **72**, 034303 (2005).
- [14] J. Reslen and S. Bose, *Phys. Rev. A* **80**, 012330 (2009).
- [15] F. Galve, D. Zueco, S. Kohler, E. Lutz, and P. Hänggi, *Phys. Rev. A* **79**, 032332 (2009).
- [16] X. Wang, A. Bayat, S. G. Schirmer, S. Bose, *Phys. Rev. A* **81**, 032312 (2010)
- [17] G. D. Chiara, S. Montangero, P. Calabrese, and R. Fazio, *J. Stat. Mech.* P03001 (2006).
- [18] H. Wichterich and S. Bose, *Phys. Rev. A* **79**, 060302(R) (2009).
- [19] P. Sodano, A. Bayat, and S. Bose, *Phys. Rev. B* **81**, 100412(R) (2010).
- [20] R. Fazio and H. van der Zant, *Phys. Rep.* **355**, 235 (2001).
- [21] L.-M. Duan, E. Demler, and M. D. Lukin, *Phys. Rev. Lett.* **91**, 090402 (2003).
- [22] S. Trotzky, P. Cheinet, S. Fölling, M. Feld, U. Schnorrberger, A. M. Rey, A. Polkovnikov, E. A. Demler, M. D. Lukin, and I. Bloch, *Science* **319**, 295 (2008).
- [23] C. F. Hirjibedin, C. P. Lutz, and A. J. Heinrich, *Science* **312**, 1021 (2006).
- [24] S. R. White and A. E. Feiguin, *Phys. Rev. Lett.* **93**, 076401 (2004).
- [25] G. Vidal, *Phys. Rev. Lett.* **93**, 040502 (2004).
- [26] S.-J. Gu, G.-S. Tian, and H.-Q. Lin, *Phys. Rev. A* **71**, 052322 (2005)
- [27] A. Bayat and S. Bose, *Phys. Rev. A* **81**, 012304 (2010).
- [28] J. Allcock and N. Linden, *Phys. Rev. Lett.* **102**, 110501 (2009).
- [29] A. Lyakhov and C. Bruder, *New J. Phys.* **7**, 181 (2005).

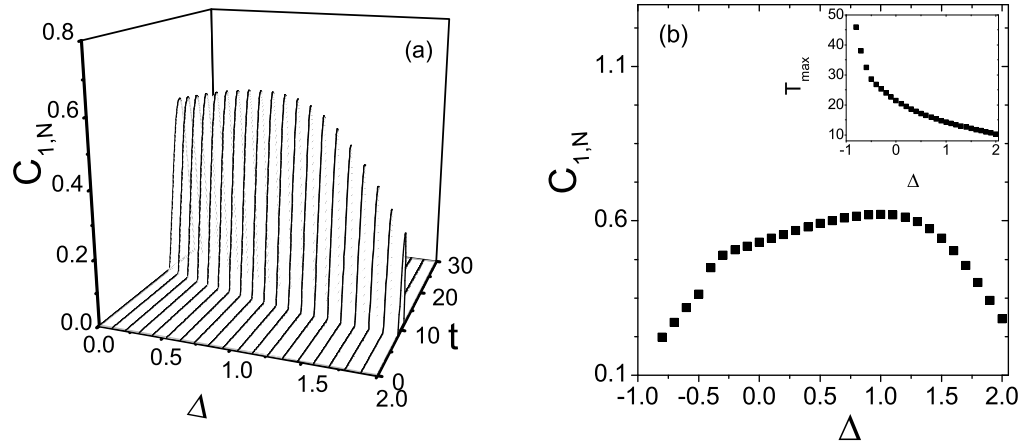


FIG. 1: (a). The long-range entanglement $C_{1,N}$ is plotted as a function of anisotropic interaction Δ and time t with $J_1 = -0.1$. The size of the system is $N = 20$. (b). The maximal value of the end-to-end entanglement is plotted as a function of the anisotropic interaction Δ . The inset shows the time of reaching the maximal end-to-end entanglement labeled by T_{max} as a function of anisotropic interaction Δ .

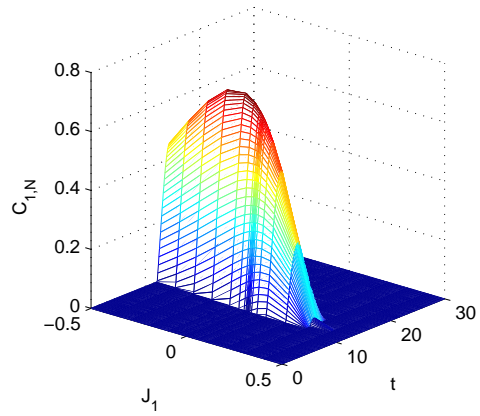


FIG. 2: The long-range entanglement $C_{1,N}$ is plotted as a function of interaction J_1 and time t when there is local quench of the interaction J_1 . The size of the system is $N = 20$ and the anisotropic interaction $\Delta = 1$. It does not include the case of $J_1 = 0$.

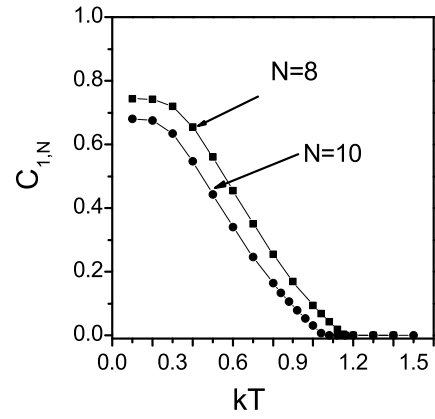


FIG. 3: The maximal value of end-to-end entanglement is plotted as a function of temperature after band quenching for different sizes.

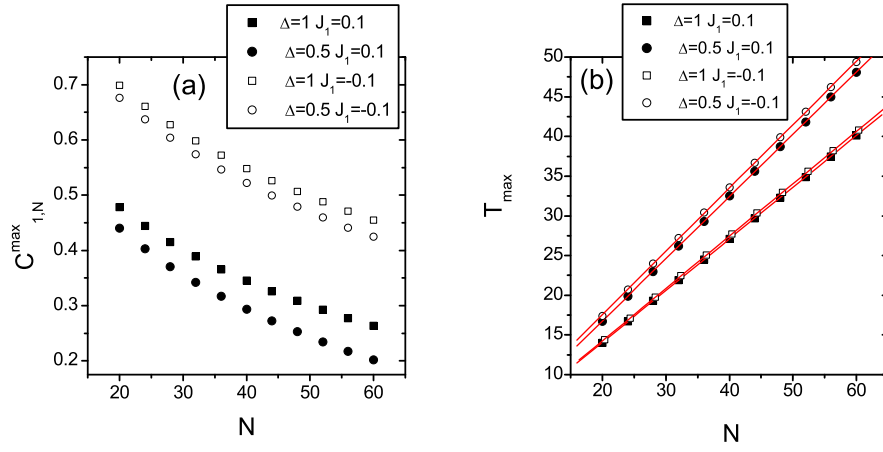


FIG. 4: (a). The maximal value of the long-range entanglement $C_{1,N}$ is plotted as a function of the size of the system for different anisotropic interaction Δ and different interaction J_1 . (b). The time of reaching the maximal long-range entanglement labeled by T_{max} is plotted as a function of the size of the system for different anisotropic interaction Δ and different interaction J_1 . The red lines are fixed lines.